Title

Preparation of photothermal palmitic acid/cholesterol liposomes

Journal

Journal of Biomedical Materials Research Part B Applied Biomaterials, 107(5)

ISSN

1552-4973

Authors

Linsley, Chase S

Zhu, Max

Quach, Viola Y

et al.

Publication Date

2019-07-01

DOI

10.1002/jbm.b.34230

Peer reviewed

Published in final edited form as:

J Biomed Mater Res B Appl Biomater. 2019 July ; 107(5): 1384–1392. doi:10.1002/jbm.b.34230.

Preparation of photothermal palmitic acid/cholesterol liposomes

Chase S. Linsley[1], **Max Zhu**[1], **Viola Y. Quach**[1], **Benjamin M. Wu**[1,2,*]

[1]Department of Bioengineering, University of California, Los Angeles, Los Angeles, CA 90095, USA

[2]Division of Advanced Prosthodontics and the Weintraub Center for Reconstructive Biotechnology, University of California, Los Angeles, Los Angeles, CA 90095, USA

Abstract

Indocyanine green (ICG) is the only FDA approved near-infrared dye and it is currently used clinically for diagnostic applications. However, there is significant interest in using ICG for triggered drug delivery applications and heat ablation therapy. Unfortunately, free ICG has a short half-life *in vivo* and is rapidly cleared from circulation. Liposomes have been frequently used to improve ICG's stability and overall time of effectiveness *in vivo*, but they have limited stability due to the susceptibility of phospholipids to hydrolysis and oxidation. In this study, non-phospholipid liposomes were used to encapsulate ICG, and the resulting liposomes were characterized for size, encapsulation efficiency, stability, and photothermal response. Using the thin-film hydration method, an ICG encapsulation efficiency of 54% was achieved, and the liposomes were stable for up to 12 weeks, with detectable levels of encapsulated ICG up to week 4. Additionally, ICG-loaded liposomes were capable of rapidly producing a significant photothermal response upon exposure to near infrared light, and this photothermal response was able to induce changes in the mechanical properties of thermally-responsive hydrogels.

Keywords

Photothermal effect; Liposome; Chromophore; Nanotechnology; Indocyanine green; Cardiogreen

INTRODUCTION

Indocyanine Green (ICG) is the only Food and Drug Administration (FDA) approved near infrared (NIR) fluorescent dye, and it is widely used clinically for diagnostic applications, such as determining cardiac output, hepatic function, and performing angiographs. Additionally, ICG has a moderate fluorescence quantum yield, and can efficiently converts light energy into heat [1,2]. This has generated interest in ICG as a candidate for thermal ablation treatments [3–5], and the photothermal response of ICG has been recently used to trigger drug release in on-demand delivery systems [6,7]. Unfortunately, free ICG has a half-life of less than four minutes *in vivo* as it is rapidly filtered from the bloodstream by the liver [8], and the optical properties of free ICG are very sensitive to factors such as solvent,

*Corresponding Author and Reprint Requests: Benjamin M. Wu, D.D.S., Ph.D. 420 Westwood Plaza, Room 5121, Engineering V. P.O. Box 951600, Los Angeles, CA 90095-1600, Fax: (310) 794-5956, benwu@ucla.edu.

concentration, and temperature [9]. Additionally, free ICG is readily hydrolyzed in aqueous medium over time [10]. To overcome these limitations, work has been done to encapsulate ICG in carriers with the aim of improving ICG's stability and overall time of effectiveness *in vivo*.

Clinical applications require that ICG remains dispersed in physiological environments, produces a strong response to light irradiation, accumulates in regions of interest, and safely resorbs into the body after use. Previous studies have shown that nano-carriers can improve a ICG's utility *in vivo*. For instance, calcium phosphate nanoparticles doped with ICG had an increase in brightness as well as prolonged signal intensity. *In vivo*, the fluorescence signal from the ICG-loaded nanoparticles was found in tumor tissue 24 hours after systemic administration, which persisted more than 96 h post-injection, while no fluorescence signal was detected from the free ICG 24 hours post-injection [11]. Liposomes are perhaps the most studied nano-carriers for ICG because they are easy to fabricate, monodisperse, and do not impact the favorable optical properties of the encapsulated chromophore [12]. To date, they have been used to demonstrate ICG's effectiveness for applications ranging from *in vivo* imaging to on-demand drug delivery [7,13–29]. Unfortunately, these liposome systems are all phospholipid-based, which have limited stability due to the susceptibility of phospholipids to hydrolysis and oxidation [30]. Recently, non-phospholipid liposomes – formed from single-chain amphiphiles and high content of sterols – have been shown to have significantly increased stability [31–34]. This increased stability suggests these liposomes systems have great potential for applications requiring long-term functionality, such as controlled drug delivery.

In this study, non-phospholipid liposomes were used to encapsulate ICG, and the resulting liposomes were characterized for size, encapsulation efficiency, stability, and photothermal response. This method utilized biocompatible and chemically inert materials – cholesterol and palmitic acid – to fabricate low-permeability liposomes comparable to those made from high sterol solutions [35]. The results show that the liposomes are stable and retain ICG for over 4 weeks and present a visible, non-aggregated, colored solution. In addition, there is a significant photothermal response of over 5°C when exposed to near-infrared (NIR) light, which was able to trigger changes in the mechanical properties of the thermally-responsive hydrogel: gelatin. Overall, the ICG-loaded liposomes reported here are fabricated using a simple liposomal formulation and have the potential to be tailored for a variety of applications, including triggered drug delivery, *in vivo* imaging and thermal ablation therapy.

MATERIALS AND METHODS

Chromophore-Loaded Liposome Fabrication

Liposomes were prepared as previously described [35]. Briefly, a solution of 3:7 molar ratio of Palmitic Acid (PA) (CAS number 57–10-3; Sigma-Aldrich, Missouri, USA): Cholesterol (CAS number 57–88-5; Sigma-Aldrich, Missouri, USA) was dissolved in 9:1 (v/v) benzene (CAS number 71–43-2; Sigma-Aldrich, Missouri, USA): methanol (CAS number 67–56-1; Sigma-Aldrich, Missouri, USA). The solution underwent liquid nitrogen flash freezing and was subsequently lyophilized for 24 hours to ensure complete sublimation of the organic solvent. The freeze-dried powder was hydrated with an aqueous ICG (CAS number 3599–

32-4; Sigma-Aldrich, Missouri, USA) solution (0.2 mg/mL, pH 8.8). The suspensions underwent five freeze/thaw cycles (liquid nitrogen for 2 min to a 70°C water bath for 10 min) with vortexing between successive cycles for good hydration. After the last cycle, the suspension was sonicated for 25 min at 20% intensity and an 80% duty cycle. A schematic of the liposome preparation is shown in Fig. 1. A Sephadex G-50 (CAS number 9004–54-0; Sigma-Aldrich, Missouri, USA) column was used to separate free ICG from ICG-loaded liposomes. Blank liposomes were also formulated using a similar procedure except substituting ICG solution with TRIS buffer (pH 8.8).

Liposome Characterization

To measure encapsulation efficiency, a 1% Triton X-100 (CAS number 9002–93-1; Sigma-Aldrich, Missouri, USA) solution was added to the purified ICG-loaded liposome solution and shaken for 10 min to lyse the liposomes. The amount of ICG encapsulated in the liposomes was measured by absorbance (700 nm) with a multi-well plate reader (Infinite® F200, Tecan Group Ltd., Männedorf, Switzerland) and compared to a standard curve of known concentrations. The encapsulation efficiency (EE) was defined as the ratio between actual versus theoretical amount of ICG encapsulated in the liposomes, as described by Equation (1). Furthermore, encapsulation efficiency was measured for liposomes exposed to single, double, or triple light exposures to see if amount encapsulated decreases with exposures.

$$Encapsulation\ Efficiency\ (EE) = \frac{actual\ amount\ of\ ICG\ loaded\ in\ liposomes}{theory\ amount\ of\ ICG\ loaded\ in\ liposomes} \times 100\% \quad (1)$$

Size and ζ-potential was measured with the Malvern Zetasizer Nano ZS model Zen 3600 (Malvern Instruments, Westborough, MA). To prepare the samples, 100 μL of chromophore-loaded liposome solution was diluted to 1 mL using distilled water. Stability studies for the liposomes followed by measuring particle diameter over 12 weeks.

Cryogenic Transmission Electron Microscopy—An aliquot of the liposome sample was dripped on a Quantifoil grid (Quantifoil R2/1 100 holey carbon films grids, Cu 200 mesh), blotted for 4 s with a manual plunger, and then plunged directly into liquid ethane. The image was collected on a FEI Tecnai TF20 at an accelerating voltage of 200 kV using TVIPS EM-Menu program (defocus = −5.0 μm, dose = 3000 e/nm^2). The instrument is equipped with a 16 megapixel CCD camera.

Photothermal Response

The experimental setup to measure the photothermal effect was conducted as previously described [6]. Briefly, 600 μL of liposome solution, diluted to 1 mL with TRIS buffer (pH 8.8), was added to a disposable cuvette that was optically transparent for visible and NIR light (780 nm). Temperature change measurements were achieved by irradiating with a POLILIGHT® PL500 multi-wavelength light source (Rofin, Australia), and a Fluke 54 Series II thermometer (Fluke Corporation, Washington, USA) was used to record the final temperature change after 2-min irradiation. The light intensity used for each

chromophore's wavelength-dependent temperature change was 750 mW and confirmed using the FieldMaxII-TO laser power meter (Coherent, California, USA). Similar to encapsulation efficiency, liposomes were tested to see if photothermal response changes with multiple exposures.

Fabrication of Gelatin Hydrogels Loaded with ICG-Liposomes

The gelatin hydrogels were prepared by dissolving bovine type B gelatin (CAS number 9000–70-8, Sigma-Aldrich, Missouri, USA) in deionized water (5 % (w/v)), and heating the mixture to 60°C until all the gelatin was in solution. The gelatin solution was removed from heat and a solution containing ICG-loaded liposomes was added. Because the gel-liquid transition temperature for palmitic acid/cholesterol liposomes is between 50–55°C [36], the gelatin solution was allowed to cool below 50°C before the liposome solution was added. Finally, the gelatin-liposome solution was transferred to the wells of a 48-well plate and allowed to set at 4°C.

Rheological Measurements

The storage modulus of the gelatin containing ICG-loaded liposomes was measured using a Discovery HR2 rheometer (TA Instruments, Delaware, USA) with an 8 mm cylindrical geometry attachment. Set gelatin hydrogels were cut-to-fit using an 8 mm biopsy punch prior to testing on the rheometer. Temperature ramps were then performed on the gelatin. The storage modulus (G') of the hydrogels were measured using a fixed strain (0.08) and angular frequency 10 rad/s. Positive control hydrogels were exposed to a 25°C to 35°C temperature ramp at a ramp rate of 2.5°C/min. Experimental hydrogels loaded with ICG-liposomes underwent oscillation-over-time tests and were exposed to 750 mW of NIR light (780 nm, Polilight PL500, Rofin, Australia) for two minutes.

The raw data was analyzed using Matlab. Briefly, a Piecewise Cubic Hermite Interpolating Polynomial (PCHIP) function performed cubic interpolation of 100 data points fitted in between the measured data points relating storage modulus to temperature for the temperature scan samples and time for the oscillation-over-time samples. The second derivative was calculated using a central derivative method and using a forward derivative method for the first data point and a backward derivative method for the last data point. The inflection point was then determined by finding the temperature at which the second derivative changes sign, indicating the melting temperature for gelatin. From the temperature ramp samples, both the melting temperature of gelatin loaded with liposomes, and corresponding storage modulus was determined. These values were used to determine if the storage modulus of melting gelatin was reached by the experimental samples exposed to NIR light, and the time of light exposure required to melt gelatin.

Statistical Analysis

Two-way repeated measures ANOVA was used to assess the temporal change in liposome diameter between ICG-liposomes and control blank liposomes. Repeated measures ANOVA was used to evaluate the results of encapsulation over time as well as the repeat light exposure experiment. Differences in the temperature change produced by ICG-liposomes and blank liposomes were compared with a two-tailed t-test, as were the differences each

group's photothermal response had on the change in gelatin's mechanical properties. The SPSS statistical software package 24.0 for Windows (IBM, Armonk, NY, USA) was used for statistical analysis. Significance was established by a value of $p < 0.05$. Data are expressed as mean ± standard deviation (SD).

RESULTS

Thin-film hydration method was used to encapsulate ICG in the palmitic acid/cholesterol liposomes with an encapsulation efficiency of 53.6% (±3.7%). The absorption peak of ICG encapsulated within liposomes exhibited a slight shift to longer wavelengths compared to free ICG in solution (Fig. 2). Specifically, the peak absorbance of the ICG liposome solution was 791 nm and the peak absorbance of the ICG solution was 780 nm. Additionally, there was an increase in visible light absorption by the ICG liposomes, which was likely due to the increase in light scattering caused by the suspended liposomes and the absorbance of the liposome materials (Supplementary Fig. 1). The amount of ICG encapsulated within liposomes decreases over time with only 43% of the initial ICG content remaining in the liposomes after 4 weeks (Fig. 3). The ζ-potential for ICG-loaded liposomes was −67.3 ± 6.7 mV, a result consistent with the deprotonated form of the carboxylate group at physiological pH. The estimated pK_a of palmitic acid in its monomeric form is 4.8, indicating that this compound will exist almost entirely in the anion form in the environment [37]. The ζ-potential for the control liposomes was −81 ± 12.5 mV. This difference was statistically significant based on a two-tailed t-test ($p=0.01$).

The liposome size was monitored over 12 weeks using dynamic light scattering analysis (Fig. 4A), and ICG-loaded liposomes were on average larger than the control liposomes with overall average diameters of 167 nm and 143 nm, respectively. Cryo-TEM of the liposomes show most are spherical unilamellar vesicles, however some multilamellar vesicles and rod-like particles are also present (Fig. 4B). A two-way repeated measures ANOVA with a Greenhouse-Geisser correction determined that mean temporal change in liposome diameter within the ICG-liposomes and control blank liposomes was not statistically significantly, and that there was no statistically significant difference between the two groups at any time point. The average polydispersity index (PDI) for both groups were low (PDI < 0.2), suggesting good uniformity, and there was no statistically significant difference in the average PDI over 12 weeks for either ICG-loaded liposomes as well as the control liposomes. Representative frequency histograms showing the size range for ICG-loaded liposomes and control liposomes are shown in Fig. 4C and 4D, respectively. Stability of the ICG-loaded liposomes in a simulated physiological environment (PBS with 10% FBS) over 7 days showed no statistically significant temporal changes in liposome diameter, but the average diameter was significantly larger (>1 μm) than liposomes in suspended in DI H_2O (Supplementary Fig. 2). It is possible that proteins screened the electrostatic interactions that stabilized the lamellar phase [38].

Aqueous solutions containing either ICG-liposomes or blank liposomes were exposed for 2 min to 750mW of NIR light, which corresponds with ICG's absorption peak. The data shows the presence of a chromophore results in a greater temperature change when compared to liposomes without ICG (Fig. 5A). Specifically, the final temperature change

of an aqueous solution containing ICG-liposomes was 5.8°C (±0.9°C), whereas the solution containing blank liposomes produced a final temperature change of 2.9°C (±0.3°C). A two-tailed t-test was conducted to compare the temperature change produced by ICG-liposomes and blank liposomes, and there was a significant difference in the temperature changes produced by the two sample types ($p<0.001$). To study the ICG-liposome's lifetime for heat generation, they underwent 3× 2 min exposures to 750mW of NIR light. The results show that ICG-loaded liposomes had no statistically significantly difference in their photothermal response between exposures as determined by one-way ANOVA (Fig. 5B). Additionally, there was no statistically significant change in liposome diameter following multiple exposures to NIR light (data not shown). The amount of ICG remaining within the liposomes decreased to 75% (±3%) of the original encapsulation after the first NIR light exposure, but between each exposure there was no statistically significantly difference in ICG content within the liposomes as determined by ANOVA with repeated measures (Fig. 5C).

Rheology was performed on gelatin hydrogels spiked with ICG-loaded liposomes and undergoing NIR light exposure to demonstrate the liposomes ability to act upon a stimuli-responsive material. First, the melting temperature of gelatin hydrogels was experimentally determined by measuring the storage modulus (G') of the hydrogels under a fixed strain (0.08) and angular frequency 10 rad/s that were exposed to a temperature ramp. The inflection point on the storage modulus graph is indicative of melting and occurred at a temperature of 30.4°C. The storage modulus at the initiation of gelatin melting was 62.1 Pa. Oscillatory testing on gelatin hydrogels exposed to 750 mW of NIR light starting at the 2 min mark showed that it took 4.3 min (± 0.8 min) to reach the melting storage modulus (Fig. 6A). Additionally, the oscillatory testing confirmed that the ICG-loaded liposomes could generate a significant temperature change (≥5°C) while embedded in a hydrogel since the experiment was conducted at room temperature (25°C). To confirm the ICG-loaded liposomes being exposed to light was causing the change in storage modulus liposomes, gelatin hydrogels loaded with blank liposomes underwent oscillatory tests. These control hydrogels did not reach the critical storage modulus even after 10 min of testing (Fig. 6B). A comparison of the storage modulus at t=4.3 min revealed that the control gels reached a storage modulus value of 195.8 Pa (±89.8 Pa; n=4), whereas the experimental gels containing ICG-loaded liposomes reached a storage modulus value of 62.5 Pa (±16.5 Pa; n=4). This difference in storage modulus was statistically significant based on a two-tailed t-test ($p=0.027$).

DISCUSSION

ICG is a popular chromophore for *in vivo* applications because it absorbs NIR light, which has significant penetration in human tissue. However, free ICG molecules are severely limited by their high clearance rate by the liver and their low stability *in vivo*, which has motivated efforts to stabilize ICG via encapsulation [8–10]. Phospholipid liposomes have been widely used to encapsulate ICG [16]. However, these liposomes suffer from poor stability due to the high reactivity of their phosphate groups. To determine if non-phospholipid liposomes prepared by thin-film hydration method are a viable way to encapsulate and stabilize ICG, the encapsulation efficiency of ICG was measured after liposome formation.

Liposome encapsulation efficiency has traditionally been a problem, as the surfactants responsible for forming liposomes require a large amount of solvent to drive liposome formation and increase entropy of the aqueous system containing the liposomes. As a result, much of the solvent, containing the dissolved drug or chromophore, is not encapsulated within the liposomes, lowering encapsulation efficiency. Many previous studies using the thin-film hydration method reported liposomal encapsulation efficiencies of around 50% [39,40]. Recent studies in encapsulating ICG are able to achieve 64% to 75% encapsulation using nanoparticles, thus avoiding the issue of excess solute remaining in the unencapsulated solvent [41,42]. However, these values are only slightly higher than the encapsulation efficiency achieved in this study. To decrease the chromophore which remains in the unencapsulated solvent, one method is to implement the dehydration-rehydration method, in which the chromophore is initially added to the liposome formulation and lyophilized alongside the lipid and surfactants used to form the liposomes [39]. Because the ICG will be infused into the thin-film lipid post-lyophilization, more ICG will be encapsulated in the liposomes upon rehydration due to proximity to the liposome film. Implementation of this procedure can perhaps further increase the photothermal response of these liposomes, as more chromophore can be encapsulated within each liposome.

The thin film of palmitic acid and cholesterol used to make the ICG-loaded liposomes was prepared using a benzene/methanol mixture. Because benzene is classified as a known human carcinogen, there is a toxicity risk for any future *in vivo* applications that use liposomes containing residual solvent. The FDA has restricted the maximum levels of residual benzene to 2 ppm [43]. In this study, the residual concentration of benzene remaining after 24 hours of lyophilization was not measured, but methods are available to measure residual solvent, such as gas chromatography [44]. In cases where lyophilization is not sufficient, modifications to the drying process can be made, such as drying for a longer time at an elevated temperature, drying under a vacuum or flow a dry gas (e.g. Nitrogen), or use methods like dialysis or gel filtration [45]. Clearly, there are several possible methods that could reduce residual solvent in the event the levels are too high for *in vivo* use.

These liposomes are relatively stable over time. Overall, the ICG-loaded liposomes are larger than the TRIS-encapsulated control liposomes, and amphiphilic ICG had a mild neutralizing effect on the ζ-potential. This size difference may also be attributed to the fact that ICG is an amphiphilic molecule with nonpolar regions. Because water molecules do not form favorable interactions with these nonpolar regions, the water near these regions lose entropy as they are locked into configurations that minimize interactions with nonpolar functional groups. To compensate, the liposomes increase in volume so that free water molecules farther away from the nonpolar regions are able to arrange in more configurations, increasing entropy internally within the liposome to compensate. After 12 weeks, the liposomes remain stable and continued to prevent chromophore aggregation. There was no visible sedimentation, and the solution was colored throughout. In contrast, control samples of free ICG solution contained chromophore sedimentation within a day. Size after NIR exposure is comparable to size prior to exposure, thus further supporting the stability of the liposomes. The low PDI further suggests a uniform distribution in diameter size. This contrasts to previous studies conducted on phospholipid liposomes, which report instability of liposomes over time due to hydrolysis of phosphate groups in the liposomes

and aggregation [7,46]. As the non-phospholipid liposomes used in this study contains low molar ratio of single-chain fatty acids, whose carboxylic acid groups are not very reactive in water, they do not experience the same problems of hydrolysis and aggregation. Thus, their size and PDI do not fluctuate over time.

The decrease in encapsulation between their formation and the first week of storage is likely due to the thermodynamics of liposome formation. Upon formation, the concentration of encapsulated ICG is high. However, as the liposomes change size while equilibrating to the most thermodynamically favorable size, encapsulated ICG is released from the liposomes and hydrolyzed in solution. Once the liposomes have reached their thermodynamically favored size, fluctuations in encapsulation efficiency decrease. These results were found to be consistent even after the liposomes were exposed to NIR light. After 4 weeks, however, there was a significant decrease in the amount of ICG encapsulated. Equilibrium would favor hydrolysis of the alkene groups in ICG, and although the rate of hydrolysis may be slow, enough hydrolysis accumulates by 4 weeks such that one can observe a significant decrease in ICG concentrations within the liposome. To further protect the ICG from hydrolysis, future studies should attempt to lower the pH within the liposome. Lowering pH will decrease the concentrations of hydroxide, which serves as the nucleophile for hydrolysis, thus decreasing the rate of hydrolysis. However, lowering pH can decrease the stability of palmitic acid/cholesterol liposomes, which relies on the electrostatic repulsion between the carboxylate groups on palmitic acid at neutral pH to mix palmitic acid among cholesterol [37,38]. Optimization experiments are required to identify conditions that maintain liposome stability while preventing chromophore degradation. Alternatively, substitution of some or all of the cholesterol with negatively charged cholesterol sulfate can help stabilize the liposomes at acidic pH values since the protonated palmitic acid help reduce interactions between the negatively charged cholesterol sulfate [37,38].

Because physiological systems do not increase in temperature by 5°C spontaneously, the ability to trigger this increase in temperature can be very useful therapeutically. Additionally, the melting temperature of the palmitic acid/cholesterol liposomes is approximately 15°C higher than physiological temperatures and the temperature change achieved by the encapsulated ICG is well below the phase transition temperature of the liposomes, which is when significant leakage of the encapsulated solute can occur [47]. Indeed, ICG-loaded liposomes were shown to produce ≥ 5°C temperature change over multiple exposures. It has been previously shown that the photothermal response of ICG irradiated with NIR is both concentration- and power-dependent and various combinations of concentrations and light-intensities can be used to meet temperature change requirements [6]. Combined with the results from the liposome stability testing, these liposomes can be used for multiple exposures for an extended period of time. Their utility is limited by the decrease in ICG encapsulated over time due to hydrolysis of the encapsulated ICG molecules. To increase the shelf life of these liposomes, the liposome solution can be lyophilized and then rehydrated before use. Studies show that although encapsulation efficiency may drop from this lyophilization and rehydration process, therapeutic effects of encapsulated molecules are increased due to decreased degradation of active drug components compared to drug-loaded liposomes that were suspended in solution over the same amount of time [46]. Creating stable and reusable chromophore-loaded liposomes proves useful for heat ablation therapies, as

a 5°C increase from physiological temperature is sufficient to trigger tissue damage from hyperthermia [48,49]. By encapsulating ICG in these liposomes, the chromophore is stable for multiple exposures to NIR light; once the liposomes have reached the affected tissue via a targeting mechanism, heat ablation can be conducted multiple times from the same injection.

The photothermal response of ICG-loaded liposomes were tested by loading liposomes into a model thermally-responsive biomaterial. Gelatin has a well-characterized melting point at 32°C and is used in various rheological studies of melting temperature [50–53]. The study monitored the storage modulus of gelatin over different temperatures, which served to indicate when the hydrogel's phase changed from solid to liquid, known as the sol-gel transition temperature. Hydrogels loaded with ICG-liposomes and exposed to NIR light consistently reached the critical storage modulus, while control gels with blank liposomes were never able to reach the critical storage modulus. The changes in the mechanical properties of the gelatin prove that the photothermal response is uniform throughout the gelatin carrier and able to create the >5°C temperature change within hydrogels.

CONCLUSION

In conclusion, non-phospholipid liposomes loaded with ICG were successfully fabricated via thin-film hydration method and demonstrated long-term stability as well as a significant photothermal response when exposed to near-infrared (NIR) light, which was able to induce changes in the mechanical properties of gelatin hydrogels. The ICG-loaded liposomes reported here are fabricated using a simple liposomal formulation and further *in vitro* and *in vivo* studies will be required to assess their potential for a variety of applications, including triggered drug delivery, *in vivo* imaging and thermal ablation therapy.

Supplementary Material

Refer to Web version on PubMed Central for supplementary material.

ACKOWLEDGMENTS

This work was supported with funding from the National Institute of Arthritis and Musculoskeletal and Skin Diseases of the National Institutes of Health (NIH) under award number R21AR064437, and from the UCLA Broad Stem Cell Research Center through the Stem Cell Research Award program. The content is solely the responsibility of the authors and does not necessarily represent the official views of the funding sponsors. Our sincerest thanks go to Dr. Zhongkai Cui from Dr. Min Lee's lab, School of Dentistry, University of California, Los Angeles, for sharing his extensive knowledge in liposome fabrication and to the lab of Dr. Gaurav Sant, Civil and Environmental Engineering, University of California, Los Angeles, for use of their rheometer. The authors also acknowledge the use of instruments at the Electron Imaging Center for NanoMachines supported by NIH (1S10RR23057) and CNSI at UCLA.

REFERENCES

1. Philip R, Penzkofer A, Baumler W, Szeimies RM, Abels C. Absorption and fluorescence spectroscopic investigation of indocyanine green. Journal of Photochemistry and Photobiology A: Chemistry 1996;96(1–3):137–148.
2. Reindl S, Penzkofer A, Gong SH, Landthaler M, Szeimies RM, Abels C, Baumler W. Quantum yield of triplet formation for indocyanine green. Journal of Photochemistry and Photobiology a-Chemistry 1997;105(1):65–68.

3. Chen WR, Adams RL, Higgins AK, Bartels KE, Nordquist RE. Photothermal effects on murine mammary tumors using indocyanine green and an 808-nm diode laser: An in vivo efficacy study. Cancer Letters 1996;98(2):169–173. [PubMed: 8556705]
4. Shafirstein G, Baumler W, Hennings LJ, Siegel ER, Friedman R, Moreno MA, Webber J, Jackson C, Griffin RJ. Indocyanine green enhanced near-infrared laser treatment of murine mammary carcinoma. International Journal of Cancer 2012;130(5):1208–1215. [PubMed: 21484791]
5. Wang GH, Zhang F, Tian R, Zhang LW, Fu GF, Yang LL, Zhu L. Nanotubes-Embedded Indocyanine Green-Hyaluronic Acid Nanoparticles for Photoacoustic-Imaging-Guided Phototherapy. Acs Applied Materials & Interfaces 2016;8(8):5608–5617. [PubMed: 26860184]
6. Linsley CS, Quach VY, Agrawal G, Hartnett E, Wu BM. Visible light and near-infrared-responsive chromophores for drug delivery-on-demand applications. Drug delivery and translational research 2015;5(6):611–24. [PubMed: 26423655]
7. Lajunen T, Kontturi LS, Viitala L, Manna M, Cramariuc O, Rog T, Bunker A, Laaksonen T, Viitala T, Murtomaki L and others. Indocyanine Green-Loaded Liposomes for Light-Triggered Drug Release. Molecular Pharmaceutics 2016;13(6):2095–2107. [PubMed: 27097108]
8. Lemmer B, Nold G. Circadian changes in estimated hepatic blood-flow in healthy-subjects. British Journal of Clinical Pharmacology 1991;32(5):627–629. [PubMed: 1954078]
9. Alander J, Kaartinen I, Laakso A, Pätilä T, Spillmann T, Tuchin V, Venermo M, Välisuo P. A review of indocyanine green fluorescent imaging in surgery. Journal of Biomedical Imaging 2012;2012.
10. Holzer W, Mauerer M, Penzkofer A, Szeimies RM, Abels C, Landthaler M, Baumler W. Photostability and thermal stability of indocyanine green. Journal of Photochemistry and Photobiology B-Biology 1998;47(2–3):155–164. [PubMed: 10093915]
11. Altinoglu EI, Russin TJ, Kaiser JM, Barth BM, Eklund PC, Kester M, Adair JH. Near-Infrared Emitting Fluorophore-Doped Calcium Phosphate Nanoparticles for In Vivo Imaging of Human Breast Cancer. Acs Nano 2008;2(10):2075–2084. [PubMed: 19206454]
12. Turner DC, Moshkelani D, Shemesh CS, Luc D, Zhang HL. Near-Infrared Image-Guided Delivery and Controlled Release Using Optimized Thermosensitive Liposomes. Pharmaceutical Research 2012;29(8):2092–2103. [PubMed: 22451250]
13. Proulx ST, Luciani P, Derzsi S, Rinderknecht M, Mumprecht V, Leroux JC, Detmar M. Quantitative Imaging of Lymphatic Function with Liposomal Indocyanine Green. Cancer Research 2010;70(18):7053–7062. [PubMed: 20823159]
14. Beziere N, Lozano N, Nunes A, Salichs J, Queiros D, Kostarelos K, Ntziachristos V. Dynamic imaging of PEGylated indocyanine green (ICG) liposomes within the tumor microenvironment using multi-spectral optoacoustic tomography (MSOT). Biomaterials 2015;37:415–424. [PubMed: 25453969]
15. Suganami A, Toyota T, Okazaki S, Saito K, Miyamoto K, Akutsu Y, Kawahira H, Aoki A, Muraki Y, Madono T and others. Preparation and characterization of phospholipid-conjugated indocyanine green as a near-infrared probe. Bioorganic & Medicinal Chemistry Letters 2012;22(24):7481–7485. [PubMed: 23122858]
16. Navarro FP, Berger M, Guillermet S, Josserand V, Guyon L, Neumann E, Vinet F, Texier I. Lipid Nanoparticle Vectorization of IndoCyanine Green Improves Fluorescence Imaging for Tumor Diagnosis and Lymph Node Resection. Journal of Biomedical Nanotechnology 2012;8(5):730–741. [PubMed: 22888743]
17. Navarro FP, Mittler F, Berger M, Josserand V, Gravier J, Vinet F, Texier I. Cell Tolerability and Biodistribution in Mice of Indocyanine Green-Loaded Lipid Nanoparticles. Journal of Biomedical Nanotechnology 2012;8(4):594–604. [PubMed: 22852469]
18. Portnoy E, Lecht S, Lazarovici P, Danino D, Magdassi S. Cetuximab-labeled liposomes containing near-infrared probe for in vivo imaging. Nanomedicine-Nanotechnology Biology and Medicine 2011;7(4):480–488. [PubMed: 21272665]
19. Zhuang Y, Ma YF, Wang C, Hai L, Yan C, Zhang YJ, Liu FZ, Cai LT. PEGylated cationic liposomes robustly augment vaccine-induced immune responses: Role of lymphatic trafficking and biodistribution. Journal of Controlled Release 2012;159(1):135–142. [PubMed: 22226776]

20. Jeong HS, Lee CM, Cheong SJ, Kim EM, Hwang H, Na KS, Lim ST, Sohn MH, Jeong HJ. The effect of mannosylation of liposome-encapsulated indocyanine green on imaging of sentinel lymph node. Journal of Liposome Research 2013;23(4):291–297. [PubMed: 23738810]
21. Zheng XH, Zhou FF, Wu BY, Chen WR, Xing D. Enhanced Tumor Treatment Using Biofunctional Indocyanine Green-Containing Nanostructure by Intratumoral or Intravenous Injection. Molecular Pharmaceutics 2012;9(3):514–522. [PubMed: 22332810]
22. Sandanaraj BS, Gremlich HU, Kneuer R, Dawson J, Wacha S. Fluorescent Nanoprobes as a Biomarker for Increased Vascular Permeability: Implications in Diagnosis and Treatment of Cancer and Inflammation. Bioconjugate Chemistry 2010;21(1):93–101. [PubMed: 19958018]
23. Zanganeh S, Xu Y, Hamby CV, Backer MV, Backer JM, Zhu Q. Enhanced fluorescence diffuse optical tomography with indocyanine green-encapsulating liposomes targeted to receptors for vascular endothelial growth factor in tumor vasculature. Journal of Biomedical Optics 2013;18(12).
24. Toyota T, Fujito H, Suganami A, Ouchi T, Ooishi A, Aoki A, Onoue K, Muraki Y, Madono T, Fujinami M and others. Near-infrared-fluorescence imaging of lymph nodes by using liposomally formulated indocyanine green derivatives. Bioorganic & Medicinal Chemistry 2014;22(2):721–727. [PubMed: 24393719]
25. Shemesh CS, Hardy CW, Yu DS, Fernandez B, Zhang HL. Indocyanine green loaded liposome nanocarriers for photodynamic therapy using human triple negative breast cancer cells. Photodiagnosis and Photodynamic Therapy 2014;11(2):193–203. [PubMed: 24657627]
26. Zhu ZQ, Si T, Xu RX. Microencapsulation of indocyanine green for potential applications in image-guided drug delivery. Lab on a Chip 2015;15(3):646–649. [PubMed: 25450664]
27. Yuan A, Tang XL, Qiu XF, Jiang K, Wu JH, Hu YQ. Activatable photodynamic destruction of cancer cells by NIR dye/photosensitizer loaded liposomes. Chemical Communications 2015;51(16):3340–3342. [PubMed: 25619336]
28. Song WT, Tang ZH, Zhang DW, Burton N, Driessen W, Chen XS. Comprehensive studies of pharmacokinetics and biodistribution of indocyanine green and liposomal indocyanine green by multispectral optoacoustic tomography. Rsc Advances 2015;5(5):3807–3813.
29. Hua J, Gross N, Schulze B, Michaelis U, Bohnenkamp H, Guenzi E, Hansen LL, Martin G, Agostini HT. In vivo imaging of choroidal angiogenesis using fluorescence-labeled cationic liposomes. Molecular Vision 2012;18(111):1045–1054. [PubMed: 22605917]
30. Grit M, Crommelin JA. Chemical-stability of liposomes - Implications for their physical stability. Chemistry and Physics of Lipids 1993;64(1–3):3–18. [PubMed: 8242840]
31. Cui ZK, Fan JB, Kim S, Bezouglaia O, Fartash A, Wu BM, Aghaloo T, Lee M. Delivery of siRNA via cationic Sterosomes to enhance osteogenic differentiation of mesenchymal stem cells. Journal of Controlled Release 2015;217:42–52. [PubMed: 26302903]
32. Cui ZK, Bouisse A, Cottenye N, Lafleur M. Formation of pH-Sensitive Cationic Liposomes from a Binary Mixture of Monoalkylated Primary Amine and Cholesterol. Langmuir 2012;28(38):13668–13674. [PubMed: 22931455]
33. Cui ZK, Lafleur M. Lamellar self-assemblies of single-chain amphiphiles and sterols and their derived liposomes: Distinct compositions and distinct properties. Colloids and Surfaces B-Biointerfaces 2014;114:177–185. [PubMed: 24184913]
34. Cui ZK, Kim S, Baljon JJ, Doroudgar M, Lafleur M, Wu BM, Aghaloo T, Lee M. Design and Characterization of a Therapeutic Non-phospholipid Liposomal Nanocarrier with Osteoinductive Characteristics To Promote Bone Formation. Acs Nano 2017;11(8):8055–8063. [PubMed: 28787576]
35. Cui Z-K, Bastiat G, Jin C, Keyvanloo A, Lafleur M. Influence of the nature of the sterol on the behavior of palmitic acid/sterol mixtures and their derived liposomes. Biochimica Et Biophysica Acta-Biomembranes 2010;1798(6):1144–1152.
36. Pare C, Lafleur M. Formation of liquid ordered lamellar phases in the palmitic acid/cholesterol system. Langmuir 2001;17(18):5587–5594.
37. Phoeung T, Aubron P, Rydzek G, Lafleur M. pH-Triggered Release from Nonphospholipid LUVs Modulated by the pK(a) of the Included Fatty Acid. Langmuir 2010;26(15):12769–12776. [PubMed: 20666419]

38. Bastiat G, Lafleur M. Phase behavior of palmitic acid/cholesterol/cholesterol sulfate mixtures and properties of the derived liposomes. Journal of Physical Chemistry B 2007;111(37):10929–10937. [PubMed: 17718556]
39. Kirby C, Gregoriadis G. Dehydration-rehydration vesicles - A simple method for high-yield drug entrapment in liposomes. Bio-Technology 1984;2(11):979–984.
40. Szoka F, Papahadjopoulos D. Procedure for preparation of liposomes with large internal aqueous space and high capture by reverse-phase evaporation. Proceedings of the National Academy of Sciences of the United States of America 1978;75(9):4194–4198. [PubMed: 279908]
41. Gomes AJ, Lunardi LO, Marchetti JM, Lunardi CN, Tedesco AC. Indocyanine green nanoparticles useful for photomedicine. Photomedicine and Laser Surgery 2006;24(4):514–521. [PubMed: 16942434]
42. Saxena V, Sadoqi M, Shao J. Indocyanine green-loaded biodegradable nanoparticles: preparation, physicochemical characterization and in vitro release. International Journal of Pharmaceutics 2004;278(2):293–301. [PubMed: 15196634]
43. Center for Drug Evaluation and Research (U.S.). Guidance for industry: Q3C tables and list. U.S. Dept. of Health and Human Services, Food and Drug Administration, Center for Drug Evaluation and Research : Center for Biologics Evaluation and Research, Rockville, MD 2017.
44. Mirmoghaddam M, Kaykhaii M, Yahyavi H. Recent developments in the determination of residual solvents in pharmaceutical products by microextraction methods. Analytical Methods 2015;7(20):8511–8523.
45. Mozafari MR. Liposomes: An overview of manufacturing techniques. Cellular & Molecular Biology Letters 2005;10(4):711–719. [PubMed: 16341279]
46. Chang HI, Yeh MK. Clinical development of liposome-based drugs: formulation, characterization, and therapeutic efficacy. International Journal of Nanomedicine 2012;7:49–60. [PubMed: 22275822]
47. Hays LM, Crowe JH, Wolkers W, Rudenko S. Factors affecting leakage of trapped solutes from phospholipid vesicles during thermotropic phase transitions. Cryobiology 2001;42(2):88–102. [PubMed: 11448111]
48. Dewhirst MW, Viglianti BL, Lora-Michiels M, Hanson M, Hoopes PJ. Basic principles of thermal dosimetry and thermal thresholds for tissue damage from hyperthermia. International Journal of Hyperthermia 2003;19(3):267–294. [PubMed: 12745972]
49. Roemer RB. Engineering aspects of hyperthermia therapy. Annual Review of Biomedical Engineering 1999;1:347–376.
50. Gilsenan PM, Ross-Murphy SB. Rheological characterisation of gelatins from mammalian and marine sources. Food Hydrocolloids 2000;14(3):191–195.
51. Bohidar HB, Jena SS. Kinetics of sol-gel transition in thermoreversible gelation of gelatin. Journal of Chemical Physics 1993;98(11):8970–8977.
52. Pang ZH, Deeth H, Sopade P, Sharma R, Bansal N. Rheology, texture and microstructure of gelatin gels with and without milk proteins. Food Hydrocolloids 2014;35:484–493.
53. Van den Bulcke AI, Bogdanov B, De Rooze N, Schacht EH, Cornelissen M, Berghmans H. Structural and rheological properties of methacrylamide modified gelatin hydrogels. Biomacromolecules 2000;1(1):31–38. [PubMed: 11709840]

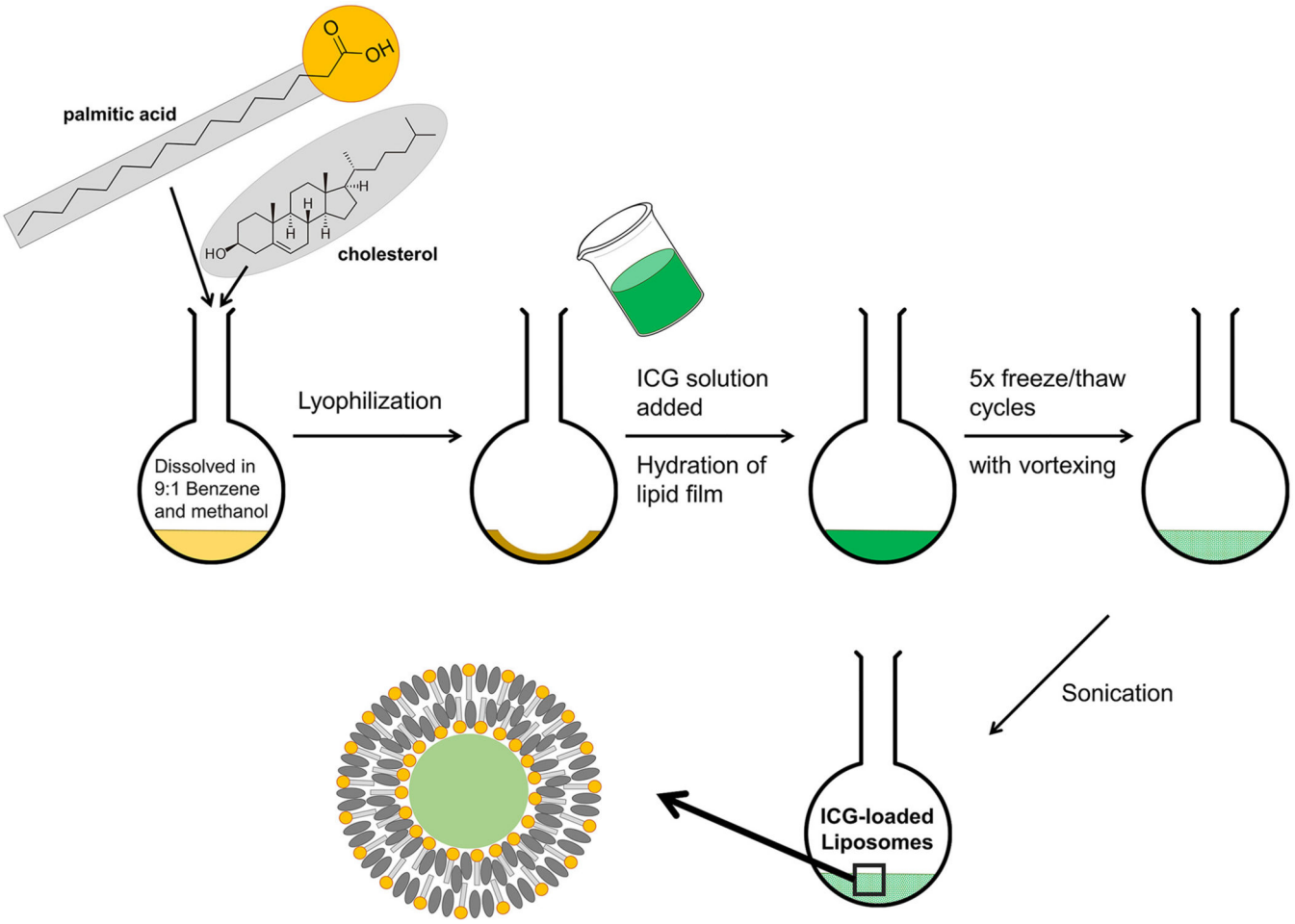

Figure 1.

Schematic of thin-film hydration method used to fabricate palmitic acid/cholesterol liposomes loaded with ICG.

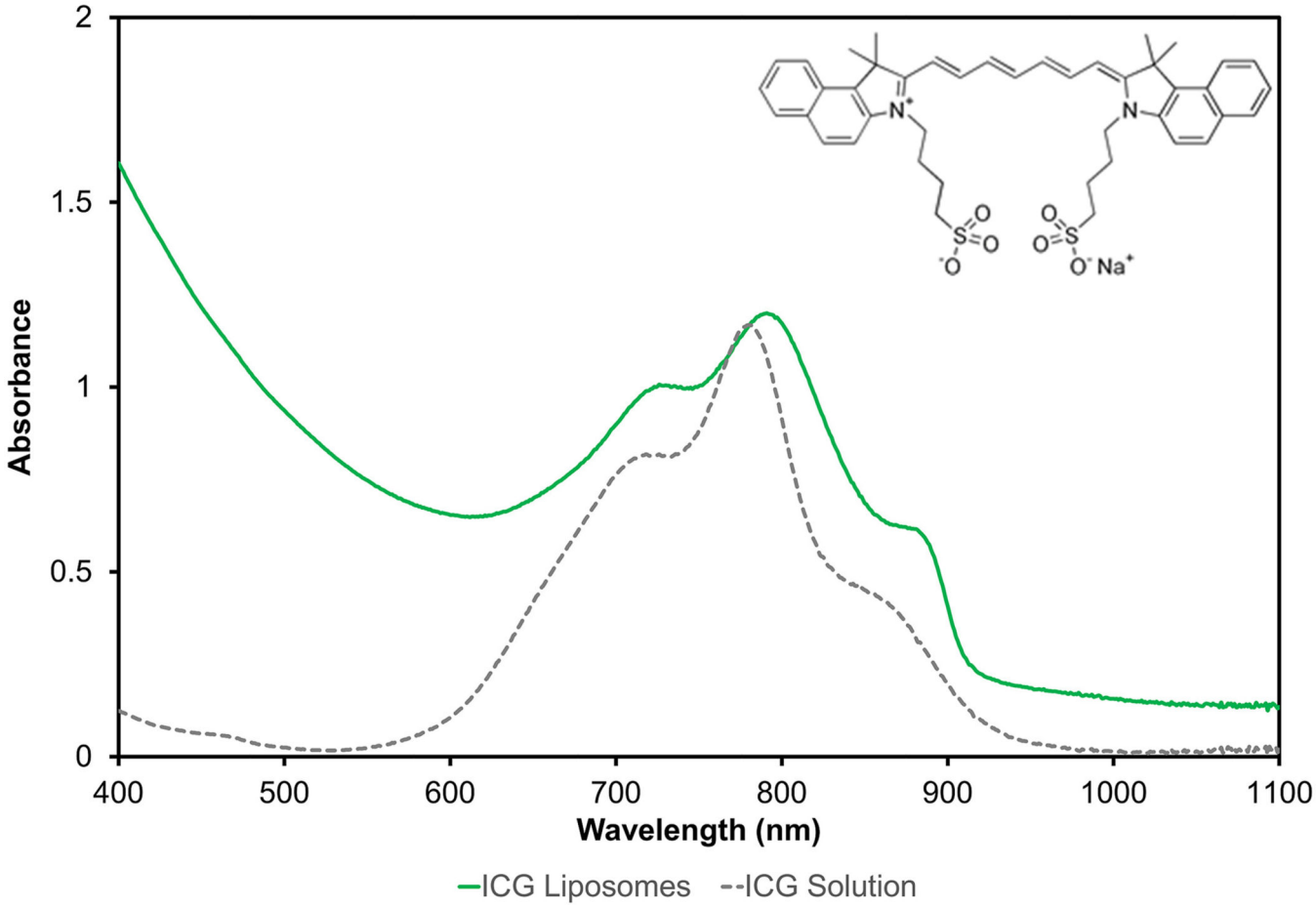

Figure 2.

The chemical structure and absorbance spectra of aqueous solutions of free ICG (0.017 μM; dashed lined) and ICG encapsulated in palmitic acid/cholesterol liposomes (solid line).

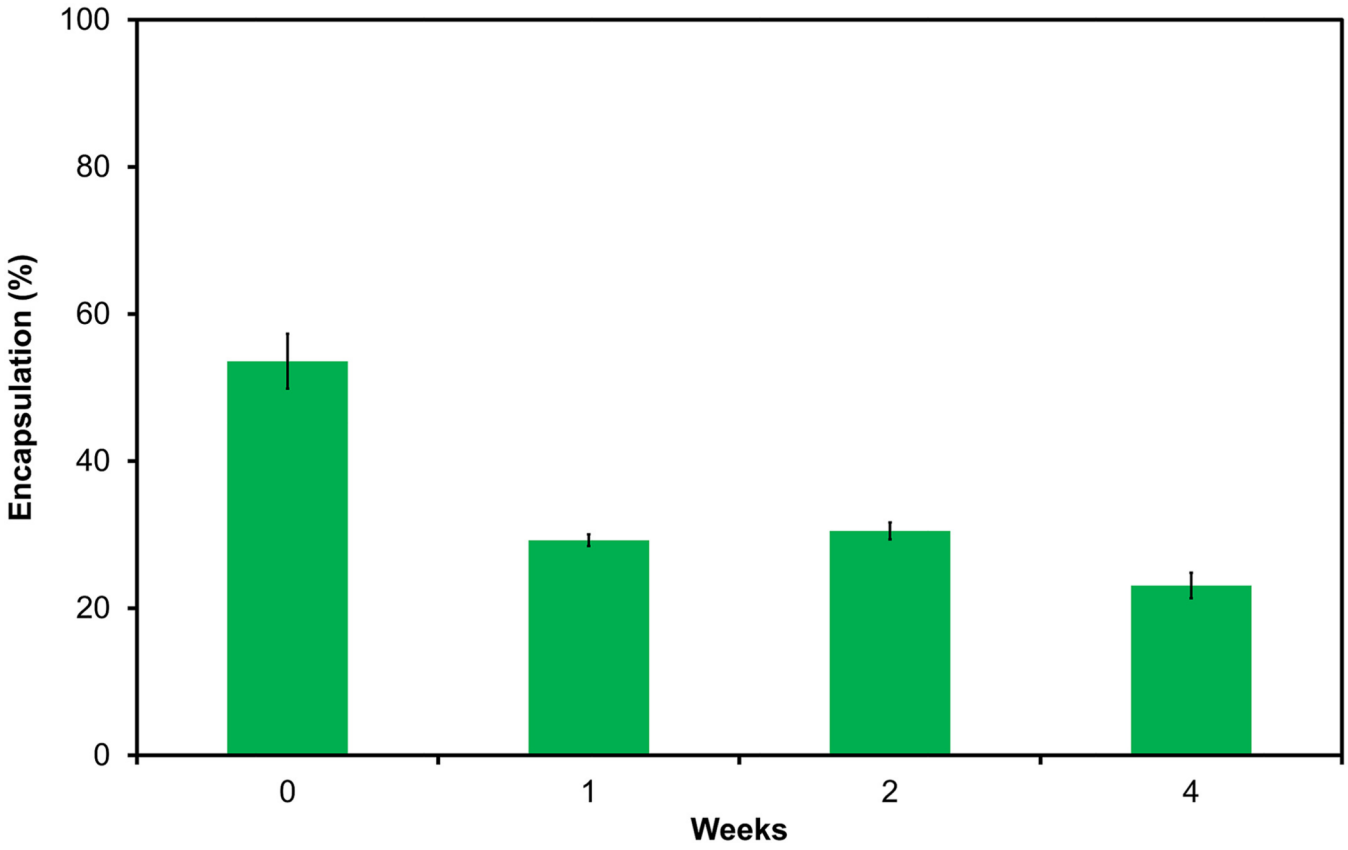

Figure 3.

Percent encapsulation of ICG within liposomes over four weeks. The encapsulation efficiency decreased from 53.6±3.7% after fabrication to 29.2±0.8% after one week. Data is presented as mean ± standard deviation (n=3).

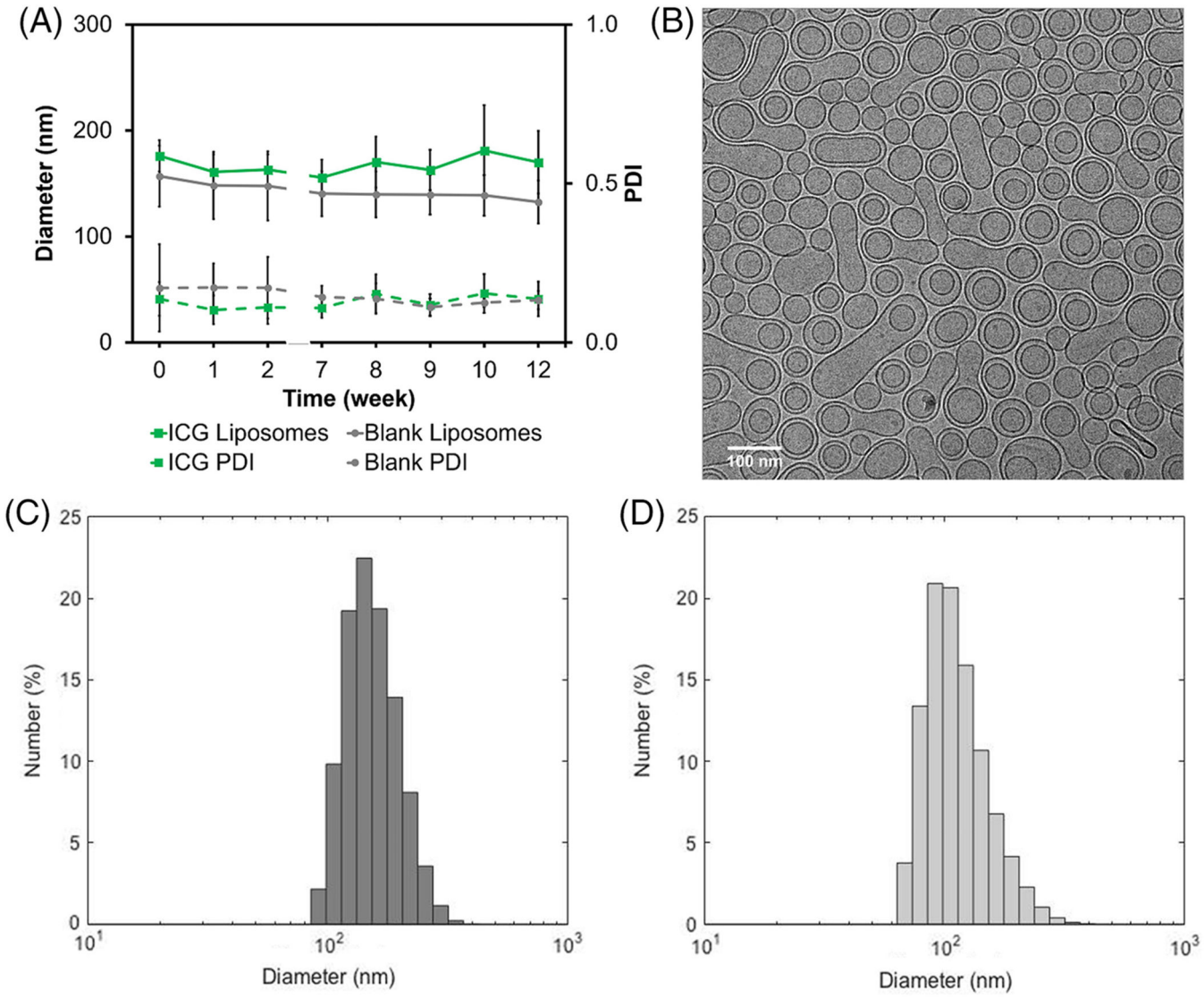

Figure 4.

A) Change in liposome diameter and PDI over time. The average diameter of ICG-loaded liposomes (■) was greater than blank liposomes (●) over the 12 weeks measured. Temporal changes in liposome diameter within the ICG-liposomes and control blank liposomes was not statistically significantly, and that there was no statistically significant difference between the two groups at any time point as determined by a two-way repeated measures ANOVA with a Greenhouse-Geisser correction (n=5). PDI measurements (dashed lines) were averaged each week, and error bars represent standard deviations. All PDI values were ≤0.30. B) Cryo-TEM image of liposomes in deionized H2O shows mostly spherical unilamellar vesicles although some multilamellar vesicles and rod-like particles were also present. Scale bar = 100 nm. Representative frequency histograms showing size range of C) ICG-loaded liposomes and D) blank liposomes at Day 0.

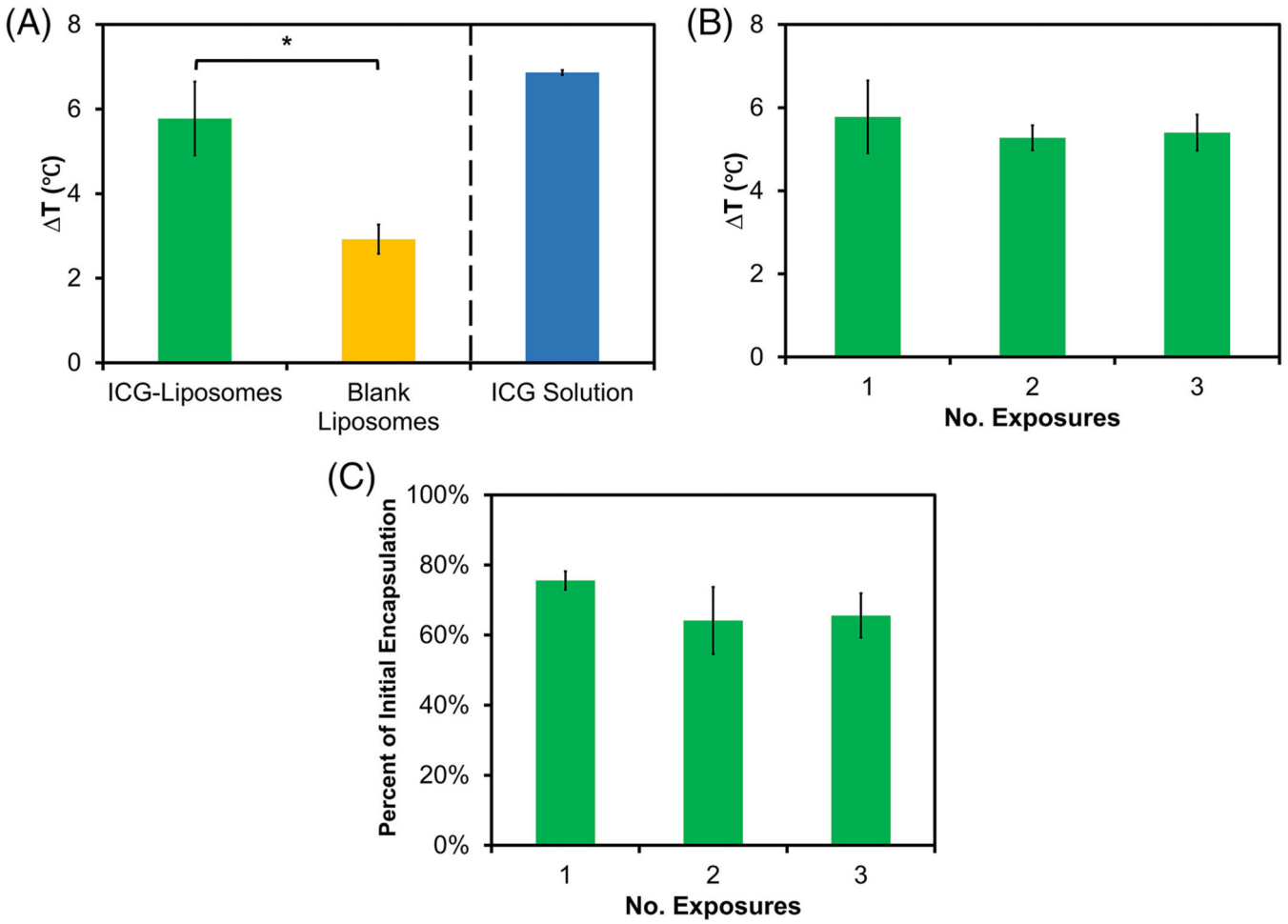

Figure 5.

A) The presence of ICG significantly increased the measured temperature change over blank liposomes (striped) upon exposure to 750 mW NIR light for two minutes (n=9). Statistical analysis performed using two-tailed t-test with significance at $p < 0.001$. Asterisks (*) indicate statistical significance between samples. The temperature change of an aqueous solutions of free ICG (13 μM) exposed to 750 mW NIR light for two minutes is shown as a reference (n=3). B) The measured temperature changes of ICG-loaded liposomes after 3× 2 min exposures to 750mW of NIR light show that ICG-loaded liposomes produce > 5°C temperature change and had no statistically significantly difference in photothermal response between exposures as determined by one-way ANOVA (n=9). C) Percent of ICG remaining encapsulated after NIR exposures. Data is presented as a percentage of initial ICG loading (Fig. 2, week 0). There was no statistically significantly difference between exposures in encapsulated ICG as determined by repeated measures ANOVA (n=9).

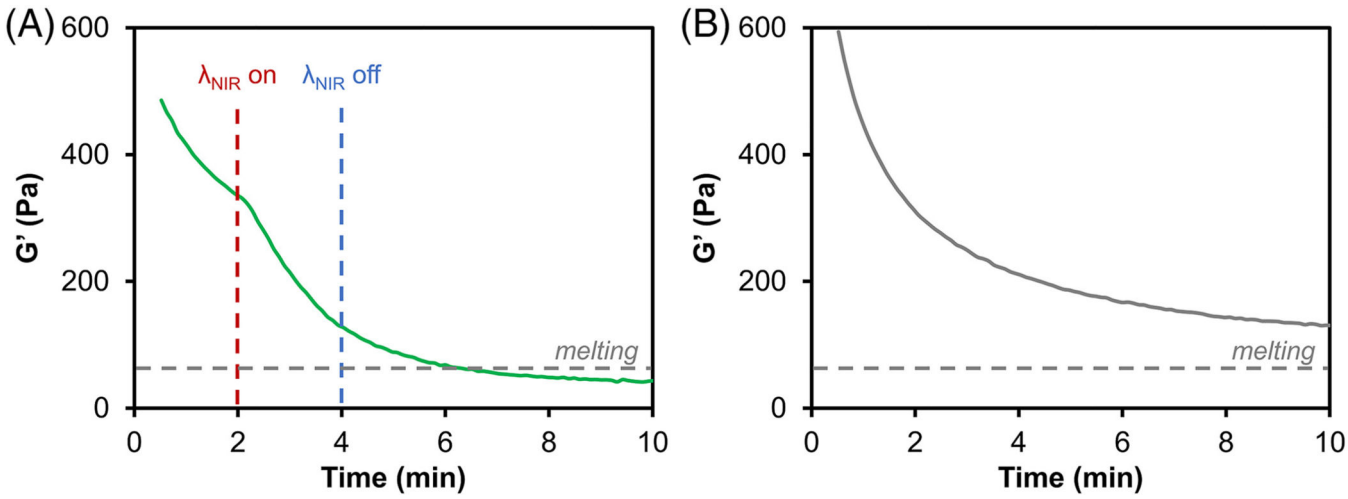

Figure 6.

Representative storage modulus vs time profiles of gelatin hydrogels with ICG-loaded liposomes (A) and blank liposomes (B). The critical storage modulus of 62 Pa was defined as the sol-gel transition point. Gelatin hydrogels with ICG-loaded liposomes that underwent NIR exposure reached that modulus 4.3 min. after exposure. Hydrogels with blank liposomes did not reach that storage modulus even after 10 min.